Comparative analysis of EspF variants in inhibition of Escherichia coli phagocytosis by macrophages and inhibition of E. coli translocation through human- and bovine-derived M cells

INFECTION AND IMMUNITY, Nov. 2011, p. 4716–4729 Vol. 79, No. 11
0019-9567/11/$12.00 doi:10.1128/IAI.00023-11

Comparative Analysis of EspF Variants in Inhibition of *Escherichia coli* Phagocytosis by Macrophages and Inhibition of *E. coli* Translocation through Human- and Bovine-Derived M Cells[▽]

Amin Tahoun,[1,2] Gabriella Siszler,[3] Kevin Spears,[1] Sean McAteer,[1] Jai Tree,[1] Edith Paxton,[1] Trudi L. Gillespie,[4] Isabel Martinez-Argudo,[5] Mark A. Jepson,[5] Darren J. Shaw,[6] Manfred Koegl,[3] Juergen Haas,[7] David L. Gally,[1]* and Arvind Mahajan[1]*

Division of Immunity and Infection, The Roslin Institute and Royal (Dick) School of Veterinary Studies, University of Edinburgh, Edinburgh EH25 9RG, United Kingdom[1]; Faculty of Veterinary Medicine, Kafrelsheikh University, Kafr el-Sheikh, Egypt[2]; Preclinical Target Development and Genomics and Proteomics Core Facilities, German Cancer Research Center, 69120 Heidelberg, Germany[3]; The Centre for Integrative Physiology, University of Edinburgh, Edinburgh EH25 9RG, United Kingdom[4]; School of Biochemistry, University of Bristol, Bristol BS8 1TD, United Kingdom[5]; Division of Veterinary Clinical Sciences, R(D)SVS and The Roslin Institute, The University of Edinburgh, Easter Bush Veterinary Centre, Roslin, Midlothian EH25 9RG, United Kingdom[6]; and Division of Pathway Medicine and Centre for Infectious Diseases, University of Edinburgh, Edinburgh EH16 4SB, United Kingdom[7]

Received 7 January 2011/Returned for modification 14 February 2011/Accepted 26 July 2011

The EspF protein is secreted by the type III secretion system of enteropathogenic and enterohemorrhagic *Escherichia coli* (EPEC and EHEC, respectively). EspF sequences differ between EHEC O157:H7, EHEC O26:H11, and EPEC O127:H6 in terms of the number of SH3-binding polyproline-rich repeats and specific residues in these regions, as well as residues in the amino domain involved in cellular localization. $EspF_{O127}$ is important for the inhibition of phagocytosis by EPEC and also limits EPEC translocation through antigen-sampling cells (M cells). $EspF_{O127}$ has been shown to have effects on cellular organelle function and interacts with several host proteins, including N-WASP and sorting nexin 9 (SNX9). In this study, we compared the capacities of different *espF* alleles to inhibit (i) bacterial phagocytosis by macrophages, (ii) translocation through an M-cell coculture system, and (iii) uptake by and translocation through cultured bovine epithelial cells. The *espF* gene from *E. coli* serotype O157 ($espF_{O157}$) allele was significantly less effective at inhibiting phagocytosis and also had reduced capacity to inhibit *E. coli* translocation through a human-derived *in vitro* M-cell coculture system in comparison to $espF_{O127}$ and $espF_{O26}$. In contrast, $espF_{O157}$ was the most effective allele at restricting bacterial uptake into and translocation through primary epithelial cells cultured from the bovine terminal rectum, the predominant colonization site of EHEC O157 in cattle and a site containing M-like cells. Although LUMIER binding assays demonstrated differences in the interactions of the EspF variants with SNX9 and N-WASP, we propose that other, as-yet-uncharacterized interactions contribute to the host-based variation in EspF activity demonstrated here.

Enterohemorrhagic *Escherichia coli* (EHEC) is an emerging zoonotic pathogen, particularly in industrialized countries (6). EHEC strains cause sporadic outbreaks of severe disease in humans, the most important being hemorrhagic colitis (HC) and hemolytic-uremic syndrome (HUS); the latter disease results in kidney damage and may lead to death (8, 28). Shiga toxins (Stx) produced by EHEC strains are the main factors responsible for these serious outcomes in humans. In contrast, Enteropathogenic *E. coli* (EPEC) is another pathogenic type of *E. coli* that can also cause severe intestinal disease in humans, although these infections are not usually associated with HC and HUS since these strains do not produce Shiga toxins. Unlike EHEC, there is no clear evidence that EPEC strains are zoonotic, although strains do circulate and cause diseases in animals (56).

* Corresponding author. Mailing address: Division of Immunity and Infection, Roslin Institute and RDSVS, University of Edinburgh, Edinburgh EH25 9RG, United Kingdom. Phone: 44 131 651 9232. Fax: 44 131 650 9232 6531. E-mail for A. Mahajan: a.mahajan@ed.ac.uk. E-mail for D. L. Gally: dgally@ed.ac.uk.

▽ Published ahead of print on 29 August 2011.

Our understanding of EHEC pathogenesis is primarily based on studies of the EHEC O157 and EHEC O26 serogroups that are associated with most human EHEC infections in Europe, North America, and Japan (39, 40, 41). Both serogroups are considered to be present in ruminants, in particular cattle as the primary reservoir (5, 41, 59, 60). Although there are many EPEC serotypes, extensive research has been carried out on the sequenced human EPEC O127 strain E2348/69. EHEC and EPEC strains express a type III secretion system (T3SS) that is important for colonization of the human or animal host (33, 36, 56, 74). The T3SS injects effector proteins into host cells that manipulate cellular processes to promote the colonization and persistence of the bacterium in the gastrointestinal tract (16, 19, 20, 34, 52, 64). The primary phenotype associated with the T3SS is intimate attachment between the bacterial outer membrane protein intimin and the T3SS translocated intimin receptor (Tir) (42). In both EHEC and EPEC, the genes encoding this protein secretion system are expressed from the locus of enterocyte effacement (LEE) pathogenicity island (33, 36). Although several effector proteins are also expressed from the LEE, a number of additional

TABLE 1. Bacterial strains used in this study

Strain	Serotype	Source
E. coli ZAP1139	O26:H11	Cattle isolate, Stx negative; Chris Low, Scottish Agricultural College, Penicuik, Scotland
E. coli TUV93-0	O157:H7	Stx phage-negative derivative of the sequenced human strain EDL933; John Leong, Massachusetts Medical School, Boston, MA (10)
E. coli TUV93-0Δ*espF*	O157:H7	This study
S. enterica serovar (SL1344) Typhimurium		Mark Jepson (38)
E. coli EPEC E2348/69 (Δ*espF*)	O127:H6	Derivative of human isolate supplied by Brendan Kenny, University of Newcastle, Newcastle, United Kingdom (74)
E. coli AAEC 185	O148	Laboratory stock
E. coli DH5α	Rough	Laboratory stock

secreted effector proteins have been identified that are expressed primarily from integrated phage elements scattered throughout the O157 chromosome (79). EHEC and EPEC strains have different combinations of effector proteins, potentially reflecting host adaptation and differences in pathogenesis.

EspF is a LEE-encoded effector protein that requires the CesF chaperone to be translocated by the T3SS into host cells (20). EspF has multiple proline-rich domains that act by binding to SH3 domains or enabled/VASP homology 1 (EVH1) domains of host cell signaling proteins (15, 55). For example, EPEC $EspF_{O127}$ binds to sorting nexin 9 (SNX9) via its SH3 amino-terminal region (1, 51). EspF is involved in disruption of tight junctions and increases monolayer permeability in part through the redistribution of occludins (54, 80). EspF sequences differ between EPEC and EHEC strains, and the EHEC O157 variant has a more modest impact on transepithelial electrical resistance (TER) (80). EspF in combination with other effectors inhibits the water transporter SGLT-1, highlighting the importance of effector interplay (16, 43). EPEC $EspF_{O127}$ is targeted to mitochondria with the N-terminal region of EspF functioning as an import signal. EPEC $EspF_{O127}$ causes an increase in mitochondrial membrane permeabilization in addition to the release of cytochrome *c* from mitochondria into the cytoplasm and subsequent caspase-9 and caspase-3 cleavage, leading to cell death (15, 58, 65, 66). More recent work has demonstrated that EspF can lead to loss of nucleolin from the nucleolus, an activity driven by EspF's activity on mitochondria (17). EPEC $EspF_{O127}$ also plays an important role in inhibition of bacterial uptake by macrophages (70), preventing macrophage phagocytosis via inhibition of the phosphatidylinositol 3-kinase (PI3K)-dependent pathway of bacterial uptake (11, 70).

Intestinal epithelium is composed of multiple cell types, including absorptive enterocytes, enteroendocrine, goblet, and Paneth cells. These cells derive through asymmetrical division migration and differentiation from pluripotent stem cells. An additional specialized epithelial cell type, termed M cells (i.e., "membranous" or "microfold" cells), are associated particularly with epithelium overlying gut-associated lymphoid tissue. This is referred to as follicle-associated epithelium (FAE) and is a site of active immunological function. In contrast to villous epithelium, FAE contains no or fewer goblet cells (67), defensin- and lysozyme-producing Paneth cells (26, 27) and expresses low amounts of membrane-associated hydrolases (68). The M cells generally lack the distinct microvilli and thick filamentous brush border glycocalyx (24) and instead have variable microfolds. Together, these features of M cells promote contact of antigens with gut epithelium and result in sampling of antigens from the intestinal lumen and transfer to antigen-presenting cells within an intraepithelial pocket (62) on its basolateral side (21, 22, 35). EPEC $EspF_{O127}$ has also been shown to inhibit EPEC translocation across antigen-transporting epithelial M cells in an *in vitro* model (53) based on a published coculture system (44).

In cattle, the terminal rectum is rich in lymphoid FAE containing M cells (49). Since this is the predominant site colonized by EHEC O157 in cattle (60), we hypothesized that EspF may have an important role in cattle colonization by inhibiting translocation of the organism by M cells and that the sequence differences of EspF in EHEC O157:H7 may reflect selection for its function in the bovine host. To test this, we compared the capacities of different *espF* alleles to inhibit phagocytosis and limit bacterial translocation through M cells derived in a coculture system to their capacities to inhibit bacterial uptake into and translocation through cells cultured from the bovine terminal rectum.

MATERIALS AND METHODS

Bacterial strains and media. EPEC, EHEC, and other *E. coli* strains used in the present study are detailed in Table 1. Bacteria were cultured in Luria-Bertani (LB) broth, minimal essential medium (MEM)-HEPES, or Dulbecco modified Eagle medium (DMEM) with antibiotics included when required at the following concentrations: chloramphenicol, 20 μg/ml; kanamycin, 50 μg/ml; and ampicillin, 100 μg/ml.

Cloning of *espF* alleles. *espF* alleles were amplified from the different strains using the primers defined in Table 2 and the products cloned into pTS1 (Table 3). BamHI and HindIII sites were used to clone the alleles from EHEC O157:H7 and O26:H11 strains. For EPEC O127 *espF*, since this contains a natural HindIII site, an alternative cloning strategy was used: pMB102 (Table 3) was digested with HindIII, followed by Klenow polymerase (Roche) treatment to create a blunt end and then restriction with BamHI. The EPEC O127:H6 *espF* PCR product was digested with BamHI and EcoRV and then cloned into the restricted pTS1. Restriction digests were set up according to the manufacturer's instructions (New England Biolabs) with the recommended enzyme buffers. All clones were checked by sequencing, and matched published database sequences for the alleles giving the amino acid sequences are shown in Fig. 2. Gateway cloning of the *espF* alleles from the different *E. coli* strains was also carried out for the LUMIER assays. *espF* alleles were amplified by using a proofreading *Taq* polymerase with the primers defined in Table 2 and cloned into the Gateway vector pDONR-207 (Invitrogen) to form entry clones. The obtained clones were checked for the correct insert by DNA plasmid extraction and restriction digestion using BanII. Once in the Gateway system, clones were easily transferred to the required destination vectors, including pTREX-DEST30 (protein A fusions) and pRenilla (luciferase fusions).

To analyze type III secretion profiles and EspF secretion from the EPEC

TABLE 2. Primers used in the study

Primer	Sequence (5′–3′)[a]	Use
EspF1F	CAGGATCCTCACAATGCAACTTAATATCG	Cloning of $espF_{O26}$ into pTS1
EspF1R	CTAAGCTTGATATAAAAAGGCATGAATTATGC	
EspF2F	CAGGATCCACCACACAATTTGATATCGGT	Cloning of $espF_{O157}$ into pTS1
EspF2R	CTAAGCTTGATATAAAGAGGCATAAATTATGC	
EspF3F	CAGGATCCACCACGCAATTTGATATCGGT	Cloning of $espF_{O127}$ into pTS1
EspF3R	CTGATATCGATATAAAGAGGCATAAATTATGC	
EspF4F	ATGCTTAATGGAATTAGTAACGC	Gateway cloning of $espF_{O157}$ and $espF_{O127}$
EspF4R	CTACCCTTTCTTCGATTGCTCATAG	
EspF5F	ATGCTTAATGGAATTAGTCAAGC	Gateway cloning of $espF_{O26}$
EspF5R	CTACACAAACCGCATAG	

[a] Restriction sites are underlined.

O127:H6 Δ*espF* and complemented strains, previous procedures were used (50, 61, 71). EspD was detected by using a monoclonal antibody kindly supplied by T. Chakraborty (Giessen, Germany). EspF was detected by using polyclonal antibodies supplied from C. Sasakawa (Tokyo, Japan) (58), and G. Hecht (University of Illinois at Chicago) (80).

Phagocytosis assays. The murine macrophage cell line (RAW 264.7) was cultured in Dulbecco modified Eagle medium (DMEM; Sigma) supplemented with 10% heat-inactivated fetal bovine serum (FBS; Sigma), 1 U of penicillin, 1 μg of streptomycin/ml, and 2 mM L-glutamine (final concentrations). Cells were grown at 37°C in 5% CO_2 and moisture. The bacteria, transformed with pUC-gfp (Table 3), were inoculated from LB broth overnight cultures into DMEM to an optical density at 600 nm (OD_{600}) of 0.3. When analyzed, the *espF* alleles were induced with 1 mM IPTG (isopropyl-β-D-thiogalactopyranoside). At an OD_{600} of 0.7, the bacterial cultures were diluted 1:5 into prewarmed DMEM, and 300 μl was added to the macrophages (initially seeded at 10^5 cells/well the day before). The cells were then incubated at 37°C in 5% CO_2 in a moist box for the desired incubation time. The cells were washed three times with sterile phosphate-buffered saline (PBS) and fixed using 4% paraformaldehyde (PFA). After three washes with PBS, the samples were incubated for 90 min with the relevant anti-lipopolysaccharide (LPS) antibody (MAST Group, Ltd.) at 1:4,000 and, after several washes, were incubated with Alexa Fluor 594-conjugated goat anti-rabbit immunoglobulins antibody (1/1,000; Molecular Probes) for an hour. The slides were then washed three times with PBS and mounted with Hydromount (National Diagnostic), and coverslips were applied. All bacteria, internal and external, express green fluorescent protein (GFP), whereas only the bacteria external to the macrophages were stained with the anti-O157 LPS antibody. This differential staining allows the proportion of internalized bacteria to be quantified.

Microscopy. Confocal data were acquired using a 1,024 by 1,024 pixel image size, a Zeiss Plan Apochromat 1.4 NA ×63 oil immersion lens, and a multitrack (sequential scan) experimental setup on a Zeiss LSM510. Image data, acquired at Nyquist sampling rates, were deconvolved using Huygens software (Scientific Volume Imaging, Netherlands), the resulting three-dimensional models were analyzed, and orthogonal views were created using NIH ImageJ software; the final figures were assembled in Adobe Photoshop.

LUMIER assays. Proteins were transiently expressed in HEK293 cells as hybrid proteins with the *Staphylococcus aureus* protein A tag or *Renilla reniformis* luciferase fused to their amino termini. Portions (20 ng) of each expression construct were transfected into HEK293 cells using 0.05 μl of Lipofectamine 2000 (Invitrogen) in 96-well plates. After 40 h, the medium was removed, and the cells were lysed on ice in 10 μl of ice-cold lysis buffer (20 mM Tris [pH 7.5], 250 mM NaCl, 1% Triton X-100, 10 mM EDTA, 10 mM dithiothreitol [DTT], protease inhibitor cocktail and phosphatase inhibitor cocktail [both from Roche], and Benzonase [Novagen]). Sheep anti-rabbit IgG-coated magnetic beads were also added (Dynabeads M280 [Invitrogen]; 2 mg/ml, final concentration), followed by incubation on ice for 15 min. Then, 100 μl of washing buffer (PBS, 1 mM DTT) was added per well, and 10% of the diluted lysate was removed to determine the luciferase activity present in each sample before washing. The rest of the sample was washed six times in washing buffer. Luciferase activity was measured in the lysate as well as in washed beads. Negative controls (nc) were wells transfected with the plasmid expressing the luciferase fusion protein and a vector expressing a dimer of protein A. For each sample, four values were measured: the luciferase present in 10% of the sample before washing ("input"), the luciferase activity present on the beads after washing ("bound"), and the same two values for the negative controls (i.e., "input nc" and "bound nc"). Normalized signal-to-noise ratios were calculated as published previously (4, 9):

TABLE 3. Plasmids used in this study

Plasmid	Description	Source or reference
pMB102	Low-copy cloning vector with inducible *lac* promoter	Tammari Schneiders, University of Belfast (69)
pAT1	pMB102 containing $espF_{O127}$	This study
pAT2	pMB102 containing $espF_{O157}$	This study
pAT3	pMB102 containing $espF_{O26}$	This study
pUC-gfp	pUC18 derivative containing *gfp*	Laboratory stock
pAJR145	*rpsM*-GFP+ transcriptional fusion in pACYC184.	Laboratory stock
pAJR146	*rpsM*-RFP transcriptional fusion in pACYC184 (pDW16) based on the DsRed T3_S4T gene	71, 76
pDONR-207	Gateway entry cloning vector	Invitrogen
pTREX-DEST30-prA	Vector to generate amino-terminal protein A fusions for LUMIER binding assays	4
pRenilla	Vector to generate amino-terminal luciferase fusions for Lumier binding assays	4
pAT4-6	$espF_{O157}$, $espF_{O26}$, and $espF_{O127}$ cloned into pTREX-DEST30-prA, respectively	This study
pAT7-9	$espF_{O157}$, $espF_{O26}$, and $espF_{O127}$ cloned into pRenilla, respectively	This study
pTREX-DEST30-SNX9 pRenilla-SNX9	Vectors expressing SNX9-protein A or -luciferase fusion proteins	This study
pTREX-DEST30-N-WASP pRenilla-N-WASP	Vectors expressing N-WASP–protein A or –luciferase fusion proteins	This study

TABLE 4. Monoclonal antibodies used in immunocytochemical screening of bovine rectal primary epithelial cell cultures

Monoclonal antibody	Specificity	Cellular expression	Source[a]	Reference
CC21	CD21	Follicular dendritic cells, mature B cells	IAH	57
CC20	Bovine CD1b	Dendritic cells	IAH	31
CC15	Bovine WC1	γd T cell	IAH	32
ILA-12	CD4	T helper cells	ILRAD	78
ILA-51	CD8	Cytotoxic T cells	ILRAD	78
ILA-156	CD40	B cells, antigen-presenting cells	ILRAD	63
ILA-111	CD25	Activated T and B cells, macrophages	ILRAD	12
ILA-43	CD2	αβ T cells, natural killer cells	ILRAD	78
Anti-hPH	β-Subunit of hPH	Fibroblasts	Acris GmbH	3

[a] ILRAD, International Laboratory for Research on Animal Diseases, Nairobi, Kenya; IAH, Institute for Animal Health, Compton, United Kingdom.

(bound/input)/(bound nc/input nc). Z-scores were then calculated using these normalized values by subtracting the population mean from an individual raw score and then dividing the difference by the population standard deviation. In normal distributions, results with a z-score of >1.96 lie within the 95% prediction interval, and z-scores of >2.58 lie within the 99% prediction interval.

Bovine primary rectal epithelial cell cultures. Bovine primary epithelial cells were derived from lymphoid dense terminal rectum 0 to 5 cm proximal to rectal-anal junction, as described previously (7, 30). Briefly, the mucosal scrapings from terminal rectum of adult cattle from a local abattoir were digested in DMEM (1% [vol/vol] fetal calf serum [FCS], 100 U of penicillin ml^{-1}, 30 μg of streptomycin ml^{-1}, and 25 μg of gentamicin ml^{-1}) containing 20 μg of dispase and 75 U of collagenase (Roche) ml^{-1}, with gentle shaking at 37°C for 90 min to release intact crypts. Crypts were enriched from contaminating gut microflora and single cells, including fibroblasts using a series of differential centrifugation steps with DMEM containing 2% sorbitol (30). Approximately 500 crypts were seeded onto collagen (Vitrogen collagen; Nutacon, Netherlands)-coated four-well chamber slides (Costar; Corning). The cells were grown to a stage of confluence (approximately 3×10^5 cells per well, typically at 5 to 7 days after initial primary epithelial cell culture). To inhibit the growth of fibroblasts, the cells were cultured in MEM–D-valine (Servichem GmbH) containing 2.5% (vol/vol) FCS, 0.25 U of insulin, 10 ng of epidermal growth factor ml^{-1}, and 25 mg of gentamicin ml^{-1} (23, 30, 46).

For the transcytosis studies, primary bovine terminal rectal epithelial cells were allowed to establish monolayers on 3-μm-pore-size polycarbonate filters of 35-mm transwell chambers (Corning Inc.) by growing them for 2 to 3 weeks until they reached confluence. Before seeding primary bovine terminal rectal epithelial cells, the transwell plates were coated with collagen (Nutagen) since it is important to establish primary cell polarization. The collagen did not block the pore, and this was checked in comparison to non-collagen-coated plates. The integrity of the cell monolayer, polarization, and formation of tight junctions was tested by measuring the TER using an epithelial voltmeter (WPI). Only filters of cell monolayers that displayed the required TER (100 Ω/cm^2) were used for the bacterial transcytosis assay. Bacteria were prepared as described for the phagocytosis assays, and 100 μl of bacterial suspension was added to each upper chamber. Bacterial counts from the lower chamber were determined at 60 min relative to the levels inoculated.

Characterization of bovine primary rectal cultured cells. The epithelial origin of the cells was confirmed by immunostaining for cytokeratin intermediate filaments. The cells at 5 days of culture were fixed with 2% PFA, permeabilized with cold acetone for 5 min, washed with PBS, and stained with a pan-cytokeratin and or anti-vimentin antibodies (Sigma, 1:300) for 3 h at 25°C. The cells were washed with PBS, and the specific monoclonal antibodies were detected using fluorescein isothiocyanate (FITC)- or TRITC (tetramethyl rhodamine isothiocyanate)-labeled secondary anti-rabbit or anti-mouse monoclonal antibody (Sigma) at 1:80. The cell nuclei were stained with TO-PRO iodide (Molecular Probes). The stained cells were mounted in fluorescence mounting medium Fluoromount (Dako) and examined by using a Leica DMLB epifluorescence microscope. To ascertain whether lymphoid cells were present in primary cell cultures from the crypts isolated from lymphoid rich mucosal tissue, immunostaining was carried out with a panel of seven monoclonal antibodies (Table 4) specific for different immune cell types of cattle.

The percentages of cells expressing vimentin in the bovine terminal rectal primary epithelial cell cultures were determined using flow cytometry. Briefly, the trypsinized cells were fixed and permeabilized in 500 μl of cell permeabilization solution (BD Pharmingen) for 10 min at room temperature. The cells were washed in PBS with 0.5% bovine serum albumin and 0.1% sodium azide. The cells were incubated with primary anti-vimentin and the respective species-specific isotype control antibodies, diluted in flow cytometry (FC) medium (DMEM, 1% FBS, 0.1% sodium azide) at 4°C for 30 min, centrifuged (2,500 rpm for 3 min), and washed twice in FC medium. The cells were then labeled with FITC-labeled secondary antibodies at 4°C for 30 min, centrifuged again, and washed twice in FC medium. The cell pellets were suspended in 200 μl of FC medium, and vimentin-expressing cells were quantified by using Calibur flow cytometer (Becton Dickinson).

Uptake of inert microparticles and *Salmonella enterica* serovar Typhimurium has been used as *in vitro* functional assay to ascertain M cells in cultures (14, 44). Similar technique was adapted to identify M-cell subsets in bovine rectal epithelial cell culture. Briefly, FITC-conjugated latex beads with a 0.2-μm pore size (Polysciences, Inc., Germany) were diluted (1:1,000) in DMEM containing 2% FBS. Aliquots (100 μl) of diluted beads were pipetted evenly onto 6-day-old cultures, followed by incubation at 37°C for 45 min; the cells were then washed three times in PBS and further incubated with *Salmonella* Typhimurium (pUC18GFP-labeled SL1344 strain) (multiplicity of infection [MOI] of 1:100) for 10 min. The cells were washed three times in PBS, fixed, and permeabilized with 2% (wt/vol) PFA–0.25% (vol/vol) Triton X-100 at room temperature for 20 min. Staining of F-actin was carried out with Phalloidin-647 (diluted 1:40 in PBS; Molecular Probes) for 45 min at room temperature. For colocalization studies with vimentin, the cells were incubated overnight at 4°C with mouse anti-vimentin monoclonal antibody (1:100; Sigma). This primary antibody was detected with Alexa Fluor 594-tagged rabbit anti-mouse or goat anti-mouse polyclonal antibodies according to the manufacturer's instructions (Invitrogen). The cell nuclei were stained with either TO-PRO iodide or DAPI (4′,6′-diamidino-2-phenylindole; Merck) nuclear stains. The mounted slides were examined by confocal microscopy. To examine the position of the beads, 0.4-μm optical sections were acquired and processed using the Imaris Surpuss module (Bitplane) computer software program.

Coculture of Caco-2 cells with Raji-B cells and measurement of bacterial translocation. Caco-2 cells were grown for 14 days in DMEM supplemented with 10% FBS, 15 mM L-glutamine, and 1% penicillin-streptomycin (Sigma) on transwell polycarbonate inserts (3-μm pore size). This time allows the differentiation and development of microvilli. These cells were then cocultured with 0.5×10^6 Raji-B cells in the basal compartment for 6 days (44). The TER was measured every day before adding the Raji-B cells until it become consistent at 200 to 300 Ω/cm^2; however, it was not changed by coculture with Raji-B cells. Bacteria were prepared as described for the phagocytosis assays, and 100 μl of bacterial suspension was added to each upper chamber. Bacterial counts from the lower chamber were determined at 60 min relative to the levels inoculated.

Kanamycin protection assay to detect intracellular *E. coli*. Bacteria were prepared as described for the phagocytosis assays. The bovine primary epithelial cells were washed twice with MEM-HEPES without antibiotic for 1 h before the bacterial culture reached an OD_{600} of 0.4, and the wells of confluent epithelial monolayer were infected by using 100 μl of bacterial suspension for each well. The infected cells were incubated at 37°C with 5% CO_2 and moisture for 1.5 h. The bacterial suspension was removed, and the wells were washed four times with PBS to remove the nonattached bacteria. A total of 500 μl of MEM-HEPES containing 750 μg of kanamycin/ml was added to each well of the infected cells. The infected cells were incubated for 3 h and then washed three times with PBS. Then, 300 μl of 0.1% Triton X-100 (in PBS) was added to each well to lyse the cells. The bacteria were collected after scraping of the cells, serially diluted in PBS, and triplicate plated onto LB plates with appropriate antibiotics. The plates were incubated at 37°C for overnight, and the colonies were counted the next day.

Statistical design and analyses. All statistical analyses were carried out in R (v2.10.1; R Foundation for Statistical Computing). All binding, uptake, and translocation assays were repeated on at least separate occasions. For all analyses, a similar methodology was adopted. Overall differences between strains were first assessed, and if there were statistically significant differences, then post hoc Tukey pairwise comparisons were carried out.

Three types of statistical models were used. Differences between strains in the percentages of intracellular bacteria at either set time intervals, as determined by fluorescence microscopy or as a measure of phagocytosis, were examined by general linear models with binomial errors to account for the percentage nature of the data. To ensure that any differences between experiments were accounted for in the time interval analysis, which of the three experiments the data came from was also entered as a covariate. When we considered differences in the number of bacteria bound per microscopic slides between the three strains, general linear models with Poisson errors were used to account for the integer nature of the data.

For all other statistical analyses, analysis of covariance of the $\log_{10}$-transformed number of bacteria posttranslocation was carried out to assess the differences between strains. To adjust for differences in pretranslocation levels and experiments, the number of bacteria pretranslocation and which of the three experiments the translocation carried out were entered as covariates. Log transformation was undertaken to normalize the residuals. Statistical significance was taken when P was <0.05.

RESULTS

Strain-specific susceptibility to phagocytosis by cultured macrophages. Previous research has demonstrated that EspF is able to inhibit bacterial uptake into macrophages, although the majority of the previous research examining this inhibition has focused on the $EspF_{O127}$ variant from EPEC O127 E2348/69. Initially, EHEC O157, EHEC O26, and EPEC O127 were compared for their capacity to inhibit their nonopsonized phagocytosis into cultured macrophages. EPEC O127 bound in significantly higher numbers to the macrophages (Fig. 1A, $P < 0.001$), and the majority remained external (Fig. 1B and C). EHEC O26 exhibited an adherence level similar to that of EHEC O157 but significantly less than that of EPEC O127 (Fig. 1A, $P < 0.001$); however, it resisted uptake by macrophages in a way comparable to that of the EPEC strain (Fig. 1B and C). In contrast, EHEC O157 adhered at lower levels, and a significantly higher proportion was phagocytosed (Fig. 1B and C). For example, at 90 min after addition 63% ± 3.3% of EHEC O157 bacteria were internalized compared to only 33% ± 3.5% of EPEC O127 or 31% ± 6.3% of EHEC O26 (Fig. 1B). By 6 h after addition to the cultures, the macrophages lost their structural integrity in the presence of EPEC O127. In contrast, macrophages exposed to EHEC were still healthy at this time point, with relatively very few bacteria evident (data not shown).

Strain-specific susceptibility to phagocytosis is associated with *espF* allele expression. EHEC and EPEC serotypes express different variants of EspF (Fig. 2). EHEC O157 contains four polyproline repeat regions (PRRs) compared to three in EPEC O127 and EHEC O26. In addition, the three sequences differ within the polyproline repeat regions and in the amino terminus of the protein shown to be important for organelle targeting (1, 17). To determine the relative contributions of the different *espF* alleles in inhibiting phagocytosis, these were amplified from *E. coli* O157, O127, and O26 and cloned into pMB102 (Table 2) under the control of a pTAC promoter that is inducible with IPTG. The sequences were confirmed to be identical to those published in the National Center for Biotechnology Information (NCBI) database for these serotypes,

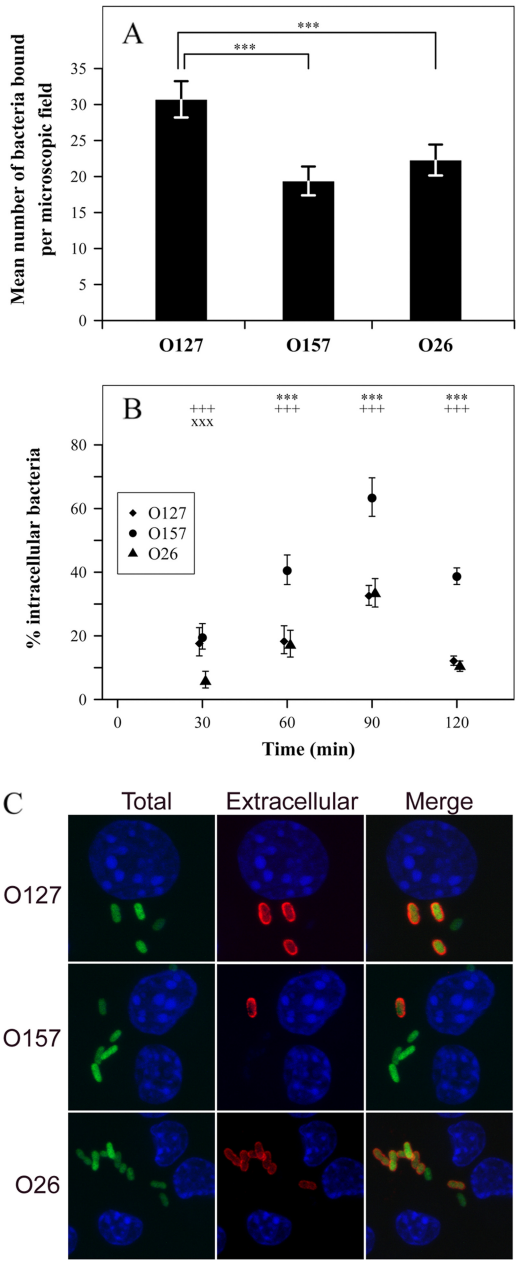

FIG. 1. Comparison of EHEC O157, EHEC O26, and EPEC O127 interactions with RAW 264.7 macrophages. Confluent monolayers of the mouse macrophages were infected with EPEC O127:H6 (E2348/69), EHEC O26:H11 (ZAP1139), and EHEC O157:H7 (ZAP1163) strains, and the number of bacteria inside (green) or outside (red) of the macrophages was determined by fluorescence microscopy as detailed in Materials and Methods. (A) Mean (± the 95% confidence intervals) numbers of adherent bacteria per macrophage at 30 min after addition of the bacteria at an MOI of 100. (B) Percentage (± the 95% confidence intervals) of intracellular bacteria at the time points shown as determined by fluorescence microscopy for EHEC O157 (●), EPEC O127 (◆), and EPEC O26 (▲). Significant differences of <0.001 for O157 versus EPEC (***), O157 versus O26 (+++), and EPEC (xxx) versus EHEC O26 are indicated. (C) Confocal images were acquired using a Zeiss Plan Apochromat 1.4 NA ×63 oil immersion lens and a multitrack (sequential scan) experimental set up on a Zeiss LSM510. Scale bar, 10 μm.

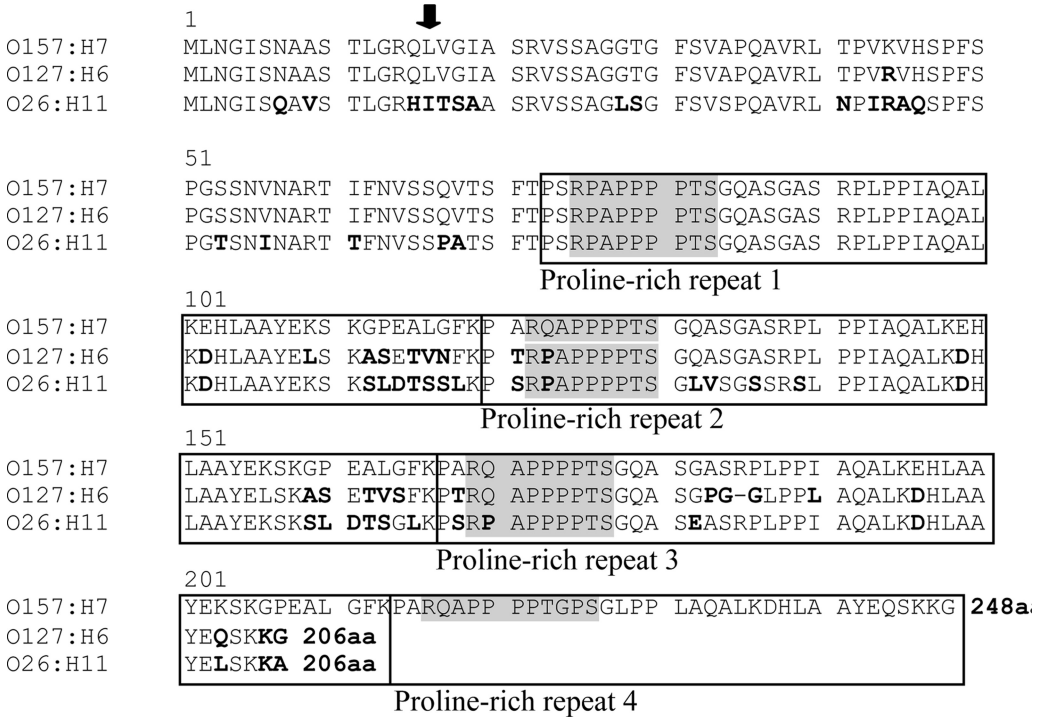

FIG. 2. Alignment of EspF amino acid sequences from EHEC O157:H7 (EDL933); EPEC O127:H6 (E2348/69), and EHEC O26:H11 (ZAP1139). The proline-rich repeats (PRRs) are boxed with EHEC O157 containing an additional fourth repeat. Amino acid differences from the EHEC O157 sequence are indicated in boldface. A binding site for SNX9 is highlighted in gray within the PRRs (1). The putative N-WASP binding region is within the middle of the PRRs (1), although the most significant sequence diversity between these variants is at the ends of each PRR. The leucine at position 16 (arrow) has been shown to be essential for EspF translocation into mitochondria, and this is changed to the similar aliphatic amino acid isoleucine in EHEC O26 (58). Analysis of NCBI *E. coli* O157:H7 sequences showed no significant variation in the predicted EspF amino acid sequence. The predicted EspF from an *E. coli* O26:H2 strain was identical to that shown for *E. coli* O26:H11 (data not shown).

resulting in the predicted amino acid sequences shown in Fig. 2. The clones were transformed into EPEC E2349/69Δ*espF* (Table 1), and the secretion profiles were examined. All strains secreted comparable levels of the translocon protein EspD; EspF secretion was detected from all three complemented strains by Western blotting (Fig. 3B) but with potentially lower levels detectable for the O26 variant. The complemented strains were then compared in a macrophage phagocytosis assay at 90 min postinfection (Fig. 3A). All three alleles were able to complement the *espF* knockout (Fig. 3, $P < 0.001$), although the *espF* gene from the *E. coli* serotype O157 ($espF_{O157}$) allele was significantly less effective at inhibiting uptake compared to the $espF_{O127}$ and $espF_{O26}$ alleles (Fig. 3A, $P < 0.001$). There were no significant differences in the adherence levels for the complemented strains (data not shown). These results indicate that the capacity of the different strains to inhibit phagocytosis correlates with the activity of the respective *espF* allele.

Strain-specific variation in M-cell translocation is associated with *espF* variation. Coculturing of human intestinal epithelial Caco-2 cells and Raji-B cells *in vitro* leads to the differentiation of a subset of epithelial cells into antigen-sampling cells (M cells) (44, 47). This *in vitro* "M-cell" culture system can then be used to analyze bacterial translocation and the capacity of bacteria to inhibit this trafficking (53). This trafficking is presumed to occur by transcytosis, but this and other research does not rule out the possibility of paracellular transport. Evidence for M-cell translocation in the assay is provided by comparison of translocation through a standard epithelial Caco-2 monolayer which occurs at significantly lower levels (Fig. 4A to C). To determine the contribution of *espF* to the translocation of EHEC O157 through this M-cell culture system, a defined deletion of *espF* was constructed in *E. coli* O157:H7 TUV93-0 (Table 1). Translocation of the EHEC O157 Δ*espF* strain was significantly higher than that of the wild-type strain across both the Caco-2/rajiB coculture and the Caco-2 monolayer. The levels of translocation were restored to those of the wild type by complementation with $espF_{O157}$ in *trans* (Fig. 4A).

The EHEC O157, EHEC O26, and EPEC O127 strains were then compared in the same coculture translocation assay. EHEC O157 demonstrated significantly higher levels of translocation compared to EPEC O127 and EHEC O26 (Fig. 4B, $P < 0.001$). To examine whether the *espF* alleles have an effect on the level of translocation inhibition, EPEC E2349/69Δ*espF* transformed with the three amplified and cloned *espF* alleles was analyzed in the same assay. All three complemented the *espF* mutation in the EPECΔ*espF* strain to a significant level (Fig. 4C, $P < 0.001$). As with the phagocytosis assay, the $espF_{O157}$ allele was the least effective of the three, being significantly less effective than the $espF_{O127}$ allele at inhibiting translocation. This was the case for translocation across both the Caco-2/Raji-B coculture and the Caco-2 monolayers, although translocation through the coculture system always occurred at significantly higher levels ($P < 0.001$). Given the

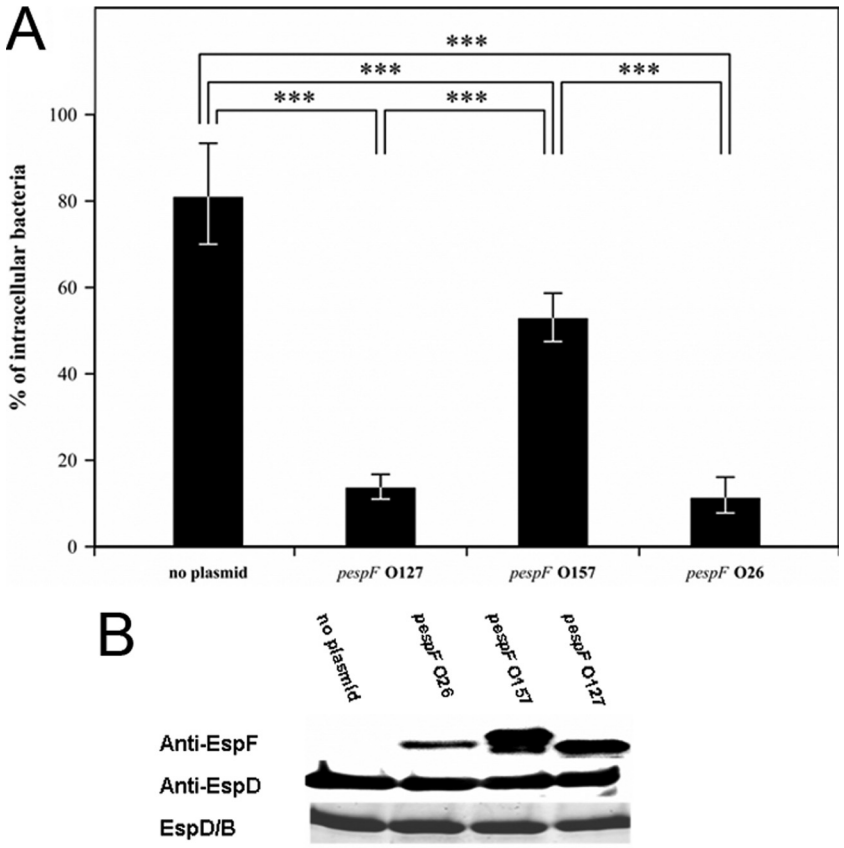

FIG. 3. Inhibition of phagocytosis (mean ± the 95% confidence intervals) by different *espF* alleles. (A) A confluent monolayer of RAW 264.7 macrophages was infected with a panel of GFP-labeled Δ*espF* EPEC strains transformed with *espF* cloned from EPEC O127:H6, EHEC O157:H7, and EHEC O26:H11. The proportions of extracellular bacteria were determined at 90 min. The infected cells were fixed in 4% PFA. Bacteria were stained with O-antigen-specific antibody detected with Alexa Fluor 594-conjugated secondary antibody. The intracellular versus total bacteria were imaged and quantified as described in Materials and Methods. ***, $P < 0.001$. (B) Levels of EspD and EspF secretion by EPEC O127 Δ*espF* and then complemented with the respective three *espF* alleles as indicated. Supernatants were prepared and separated in a standard sodium dodecyl sulfate denaturing gel that was then stained with colloidal blue. The bottom panel shows the staining for the main EspD/B band. The middle panel shows the same samples with detection for EspD. The top panel shows the detection of EspF. The supernatants were prepared from equal volumes of bacteria (50 ml) cultured to an OD_{600} of 0.8. Experimental details are given in Materials and Methods.

correlation with strain origin, these differences again indicate variation in EspF activity between the different *espF* alleles.

The significance of *espF* alleles on the interaction of *E. coli* with primary cultures of bovine rectal epithelial cells. Previous work has established that EHEC O157:H7 colonizes the terminal rectum of cattle, the main reservoir host (60). The tissue at this site contains a high number of lymphoid follicles and M-like cells that are present in the FAE (49). Primary cells were cultured from a mixed population of crypts isolated from this bovine terminal rectum (see Materials and Methods). The cells in the monolayers expressed cytokeratins (Fig. 5A) indicative of epithelial cells. Screening with a panel of antibodies (Table 4) provided no indication of contaminating cells, such as fibroblasts (data not shown). It was apparent that a small proportion of cells expressed vimentin, an intermediate filament protein indicative of M cells (Fig. 5A and B). A subset of vimentin-expressing cells endocytosed latex fluorescent microparticles (Fig. 5C and C1). *S. enterica* serovar Typhimurium preferentially targets M cells in the gut (14) and therefore was used to test whether the bacteria and the latex particles were internalized by vimentin-expressing cells in culture. Indeed, during early stages of infection, *Salmonella* Typhimurium interacted primarily with vimentin-expressing cells in culture (Fig. 5D) that also had internalized the latex beads (Fig. 5E), a further indication that these cells can be considered M cells based on previous M-cell characterization studies (44). Taken together, these data indicate that primary cells cultured from crypts isolated from bovine rectal FAE do contain a subset of cells with characteristics of M cells and are capable of taking up particles, including bacteria.

To determine the significance *espF* has on the interaction of *E. coli* O157 with these primary cells, translocation across these primary cell cultures was then assessed for the wild-type strains, the EHEC O157 Δ*espF* deletion, and EPEC Δ*espF* strain complemented with the three different alleles. In agreement with the coculture translocation assay, *espF* significantly contributed to inhibition of translocation through these cultured cells (Fig. 6A); however, in clear contrast to the "human" coculture system, EHEC O157 was significantly better in the bovine assay at inhibiting translocation compared to EPEC O127 and EHEC O26 ($P < 0.001$) (Fig. 6B). In agreement with this, the $espF_{O157}$ allele showed the highest activity in restrict-

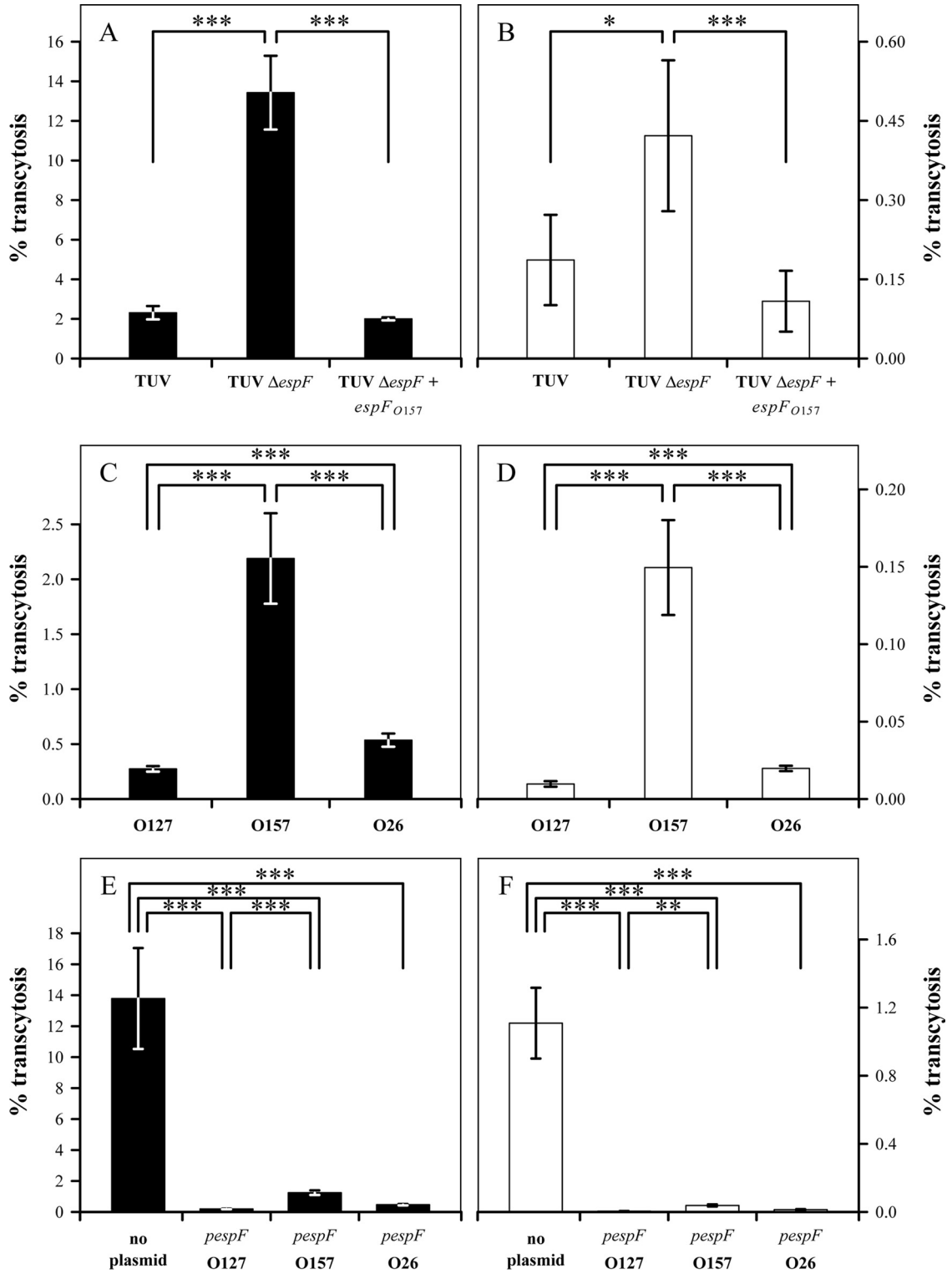

FIG. 4. Translocation of EPEC and EHEC strains across a Caco-2 and lympho-epithelial M-cell coculture system (black columns [A, C, and E]) and Caco-2 cells only (white columns [B, D, and F]). (A and B) *espF* is required to inhibit EHEC O157 TUV93-0 translocation through M cells. The translocation of EHEC O157 TUV93-0 was compared to an isogenic *espF* deletion mutant and complemented with $espF_{O157}$ (pAT1, Table 2). (C and D) Comparative translocation of EPEC O127:H6 strain E2348/69, EHEC O157:H7 ZAP198, and EHEC O26:H11 across the coculture system. (E and F) Comparative translocation of an EPEC O127Δ*espF* mutant complemented with the three defined *espF* alleles. *, **, and ***, statistical significances of $P < 0.05$, $P < 0.01$, and $P < 0.001$, respectively.

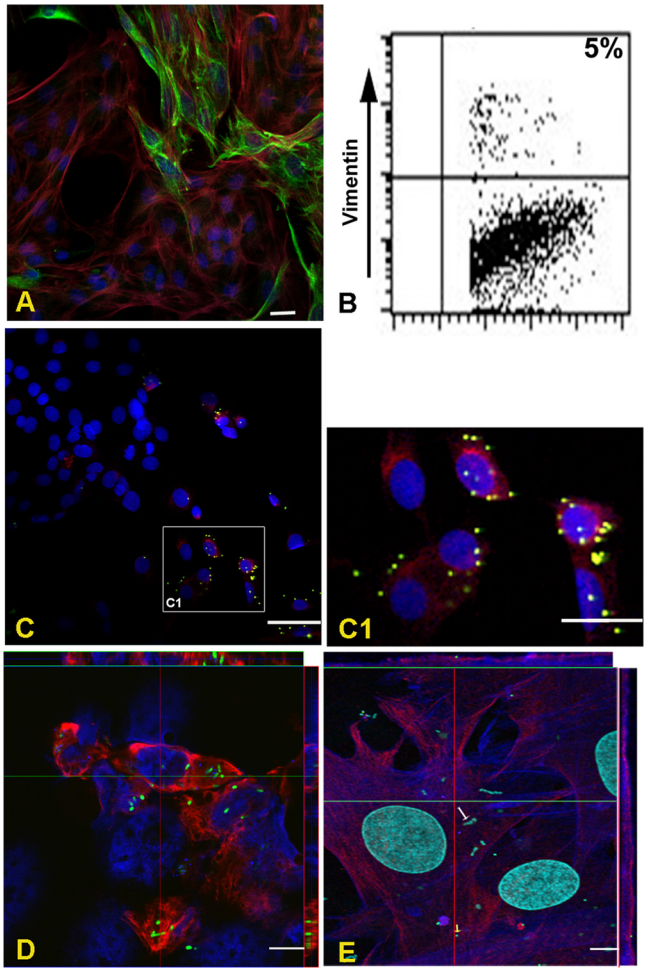

FIG. 5. Characterization of bovine primary rectal epithelial cells. (A) Heterogeneous population of epithelial cells in a primary cell culture from the bovine terminal rectum. A 5-day-old culture was prepared and immunolabeled to detect vimentin (green), pan-cytokeratins (red), and nuclei (blue) as described in Materials and Methods. A subset of the cells expressed the intermediate filament protein, vimentin (green), which is indicative of M cells. (B) Vimentin-expressing cells were quantified by using flow cytometry from four independent primary cultures (standard deviation, ±0.3). (C) Microparticle colocalization with vimentin-expressing cells. A subset of vimentin expressing (red) cells interacted with fluorescent microparticles (green). Panel C1 shows the inset image in panel C digitally magnified by a factor of 4. The primary rectal epithelial cells were incubated with latex particles (green, 0.2 μm in size) at 37°C and 5% CO_2 for 45 min, fixed, permeabilized, and labeled with anti-vimentin (red) and TO-PRO nuclear stain (blue). (D) Orthogonal section demonstrating *S. enterica* serovar Typhimurium uptake by vimentin-expressing cells during the early stages of interaction. The cells were infected with mid-log-phase *S.* Typhimurium (pUC18GFP-labeled SL1344 strain) at an MOI of 1:100 at 37°C and 5% CO_2 for 10 min. (E) Orthogonal section demonstrating the combined uptake of *S.* Typhimurium (white arrow, DAPI stained) and microparticles (yellow arrow, green) by vimentin-positive cells (red) in a bovine rectal primary culture. The cells were incubated with latex particles (green) for 45 min, washed (3× PBS), and further infected with mid-log-phase *S.* Typhimurium at an MOI of 1:100 for 10 min. The infected cells were fixed and labeled with anti-vimentin (red) and DAPI nuclear stain. Confocal images were acquired by using a Zeiss LSM510 with a ×63 objective lens). Scale bar, 10 μm.

ing transcytosis in the EPEC Δ*espF* background, although this was not significant (Fig. 6C) compared to the two other alleles. As an alternative assessment of the function of these alleles on the bovine primary cells, an intracellular kanamycin protection assay was developed that determined the intracellular bacterial numbers at 90 min postinfection. The relative percentage of bacteria taken up into cells is low but increased significantly upon deletion of *espF* (Fig. 7A). EHEC O157 was taken up into cells at significantly lower levels compared to EPEC O127 and EHEC O26 (Fig. 7B, $P < 0.001$) in agreement with the transcytosis results. This assay was then carried out with the three *espF* alleles in the EPEC E2348/69Δ*espF* strain. All three *espF* alleles reduced uptake significantly (Fig. 7C, $P < 0.001$) with the $espF_{O157}$ variant showing significantly higher activity than the $espF_{O127}$ ($P < 0.05$) and $espF_{O26}$ ($P < 0.001$) alleles (Fig. 6E).

The fact that the relative activities of the *espF* clones are reversed in the bovine assays indicates that the differences measured between the variants are not due to expression or secretion levels. This is supported by the correlations with the relative activity levels of the parental strains in the different assays. Taken together, it is likely that the relative activities are due to different functional capacities of the EspF variants and, in turn, these are dependent on the host cell type in which the variants are acting.

Molecular basis to the comparative activity of EHEC and EPEC *espF* alleles. Previous work has established that EspF has a number of interacting partners in eukaryotic cells including interactions with both sorting nexin 9 (SNX9) and N-WASP. Since SNX9 is important for endocytosis dynamics and N-WASP is central to actin polymerization, we investigated by LUMIER binding assay whether differences in the interactions of the EspF variants with these proteins could account for the differences in functional levels measured in the present study. To quantify the binding activity, the three EspF variants, as well as their binding partners SNX9 (human) and N-WASP (human), were cloned into plasmids that express either protein A-tagged proteins or *Renilla* luciferase fusion proteins as described in Materials and Methods. Cell lysates containing both sets of tagged proteins were generated, and then the protein A-tagged complexes were removed by using antibody-coated beads. Total fluorescence and captured fluorescence were measured and normalized, and z-scores for each interaction were determined as outlined in Materials and Methods and as previously published (4). The results confirmed the interaction of all of the EspF variants with both SNX9 and N-WASP (Fig. 8). The $EspF_{O157}$ had the lowest interaction score of the three variants with luciferase-linked SNX9 and also had the lowest interaction score of the three with respect to binding to N-WASP.

DISCUSSION

EPEC is known to inhibit phagocytosis via inhibition of PI3K activity, and this has been shown to be due to the activity of the type III-secreted effector EspF (11, 70). Although more recent research has established that a number of secreted proteins can also function to inhibit uptake into cells, including EspB (34), EspJ (52), and EspH (18). The inhibition of EPEC translocation through M cells has been shown to be dependent

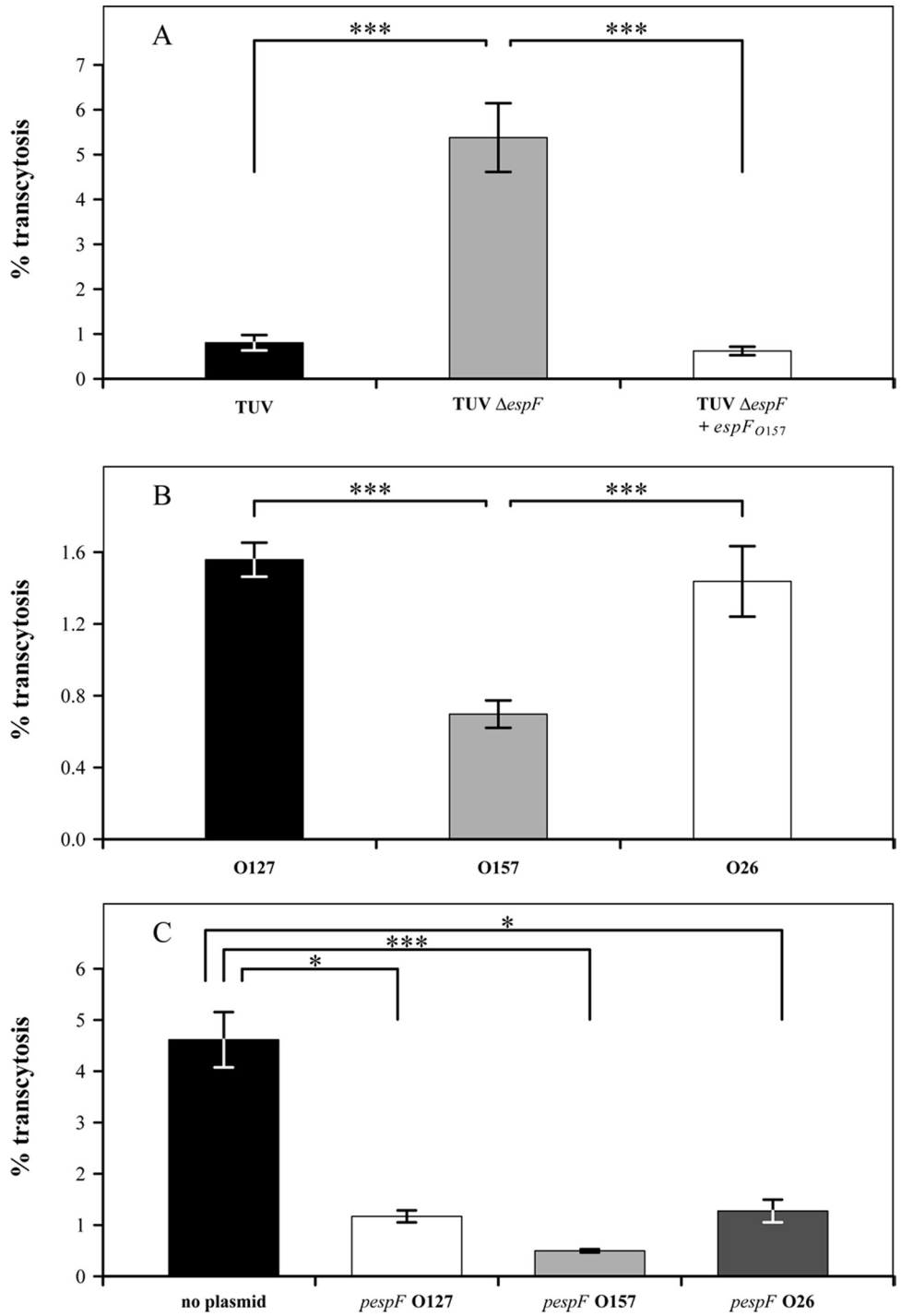

FIG. 6. Interaction of EHEC and EPEC strain with cultured epithelial cells from the bovine terminal rectum. (A) *espF* limits EHEC O157 TUV93-0 uptake into rectal primary cells. The transcytosis levels (%) of EHEC O157 TUV93-0 were compared to an isogenic *espF* deletion mutant and complemented with *espFO157* (pAT1, Table 2).(B) Comparative transcytosis levels (%) of wild-type strains EPEC O127:H6 E2348/69, EHEC O157:H7 TUV93-0, and EHEC O26:H11 on interaction with bovine rectal primary cells. (C) Comparative transcytosis levels (%) of an EPEC O127Δ*espF* mutant complemented with the three defined *espF* alleles. ∗ and ∗∗∗, statistical significances of $P < 0.05$ and $P < 0.001$, respectively.

on *espF*, presumably in a manner analogous to its activity on macrophages. Comparison of EspF protein sequences from EPEC O127, EHEC O26, and EHEC O157 shows a number of differences in both the localization domain and in the number and sequence of proline-rich repeats (PRRs). The aim of the present study was to investigate whether these differences affected the capacity of the EspF variants to (i) inhibit bacterial phagocytosis into macrophages, (ii) inhibit M-cell translocation in a human-derived Caco-2/Raji-B coculture system, and (iii) inhibit uptake into bovine primary epithelium, containing

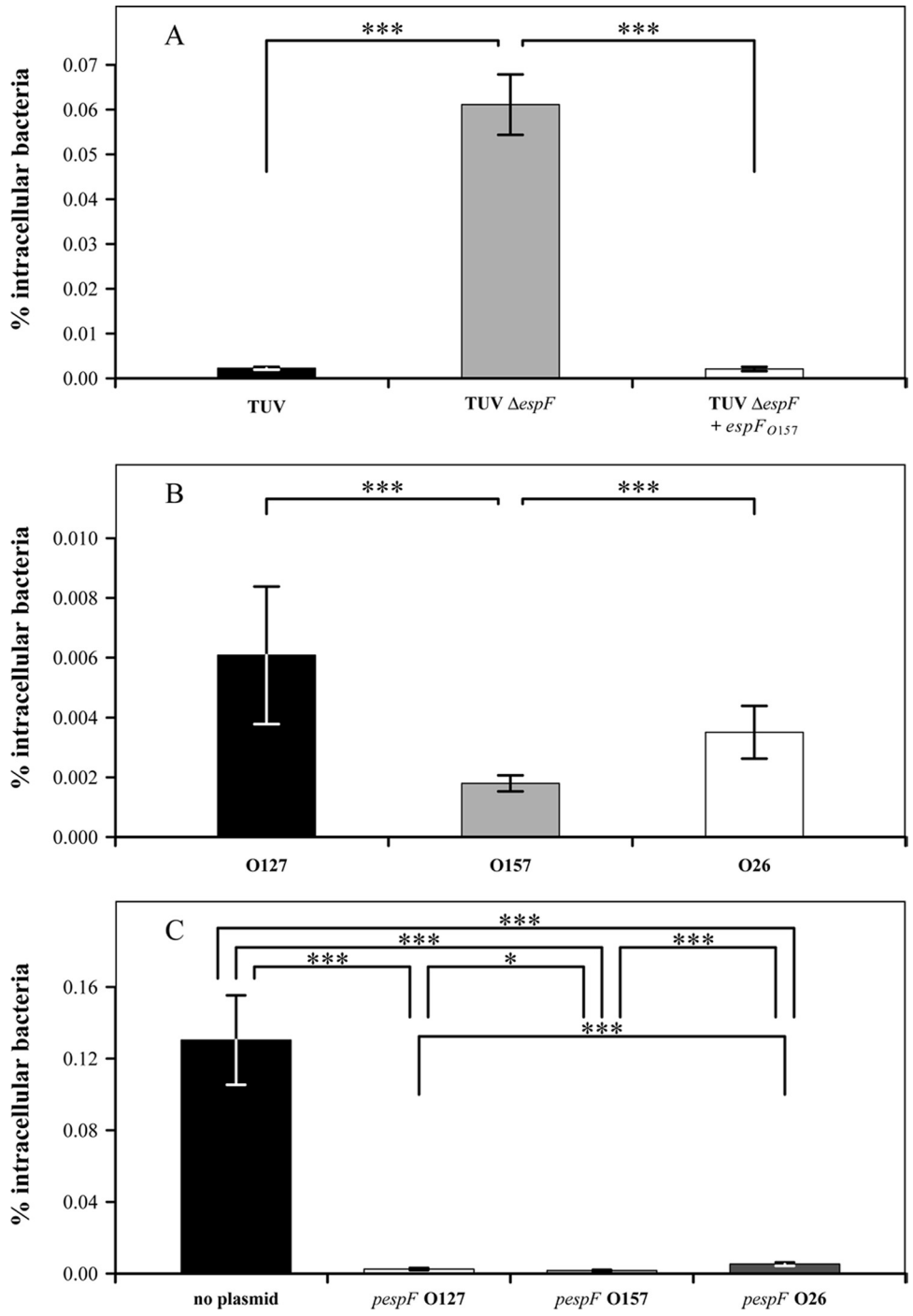

FIG. 7. Interaction of EHEC and EPEC strain with cultured epithelial cells from the bovine terminal rectum. (A) *espF* limits EHEC O157 TUV93-0 uptake into rectal primary cells. The intracellular levels of EHEC O157 TUV93-0 were compared to an isogenic *espF* deletion mutant and complemented with $espF_{O157}$ (pAT1, Table 2). (B) Comparative intracellular levels of wild-type strains EPEC O127:H6 E2348/69, EHEC O157:H7 TUV93-0, and EHEC O26:H11 on interaction with bovine rectal primary cells. (C) Comparative intracellular levels of an EPEC O127Δ*espF* mutant complemented with the three defined *espF* alleles. * and ***, statistical significances of $P < 0.05$ and $P < 0.001$, respectively.

M-like cells, cultured from the terminal rectum of cattle, the predominant colonization site of EHEC O157:H7 in cattle.

Strain comparisons demonstrated that both EPEC O127 E2348/69 and *E. coli* O26:H11 had a much greater capacity to block nonopsonized phagocytosis into cultured murine macrophages compared to EHEC O157:H7. Both the EHEC O157 and the EHEC O26 strains adhered to the macrophages at lower levels than the EPEC O127 strain (Fig. 1). To determine whether this strain difference could be accounted for by variation in the EspF effector protein, the genes from the three

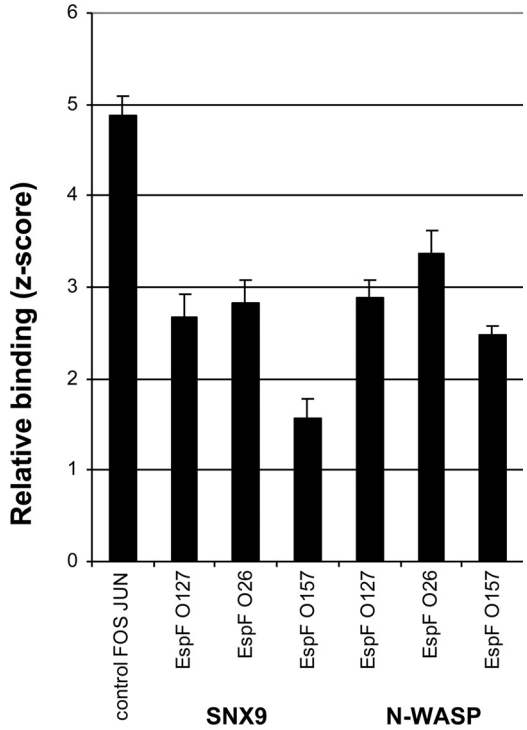

FIG. 8. Comparative binding analysis between EspF variants and human SNX9 or N-WASP. In the LUMIER binding assay, the *espF* alleles were expressed with a protein A tag and then immobilized on immunoglobulin beads. The interaction between proto-oncogenes, c-Fos and c-Jun, was used as a positive control. SNX9 and N-WASP were expressed with *Renilla* luciferase tags and incubated with the immobilized EspF variants. The luminescence signals were determined and normalized against negative controls, and z-scores were calculated as described previously (4, 9) and in Materials and Methods.

serogroups, EPEC O127, EHEC O157, and EHEC O26 were cloned and expressed in EPEC O127 from which *espF* had been deleted. Although the *espF* alleles from both O127 and O26 completely complemented the mutant, the $espF_{O157}$ allele showed a significantly reduced ability to block phagocytosis. This indicates that the initial strain observations may be accounted for by differences in the *espF* alleles. This result does not rule out important antiphagocytic functions for the other effector proteins but does indicate synergistic roles with EspF and a significant dependence on EspF. The different alleles did not alter the level of attachment of the complemented EPEC strain to Caco-2 cells, a finding in line with previous research indicating that EspF has no direct role in attachment and attaching/effacing lesion formation (55, 61, 74).

It was then investigated whether the different *espF* alleles varied in their capacity to inhibit *E. coli* translocation through M cells. The rationale for investigating this function is the finding that EHEC O157:H7 predominantly colonizes the terminal rectum of its main reservoir host, cattle, and that this site is rich in lymphoid follicles (60). Epithelium associated with lymphoid follicles is subject to different signals from the high abundance of B and T cells in these follicles leading to production of M cells (44) that sample lumen particles from the gut, delivering them to antigen-presenting cells that initiate appropriate adaptive immune responses at these sites. M cells have been postulated to be an important cell for the initial uptake or colonization by different enteric bacterial pathogens such as *Salmonella*, *Shigella*, and *E. coli* (37, 45). For EHEC O157:H7, it is a cell type that the bacteria will encounter when colonizing the terminal rectum (49, 60) and, consequently, inhibiting translocation may promote colonization, for example, by providing an initial attachment site and/or limiting bacterial presentation to the host's immune system. The origin of M cells is unclear since studies either support their derivation from enterocytes via extrinsic stimuli (luminal antigens and/or lymphoid-follicle derived signals) or conclude that they originate from lineage-specific precursor cells (25, 72, 73, 75). An M-cell coculture system was first defined in 1997 (44) and makes use of the capacity of Raji-B cells to signal differentiation of human colon-derived Caco-2 cells. Initial experiments demonstrated that *espF* from EHEC O157 is required to limit EHEC O157 translocation through M cells but that the EHEC O157 *espF* allele was again reduced in its capacity to limit translocation of *E. coli* compared to the O127 and O26 alleles. This finding mirrored the relative capacity of the specific strains to inhibit their translocation, again demonstrating the significance of the *espF* allele for the strain phenotype.

The strains and *espF* alleles were then compared on primary cells cultured from crypts isolated from the bovine terminal rectum. These cultures were further characterized in the present study. A subset of the primary cells expressed the intermediate filament protein, vimentin, that is found in rabbit intestinal M cells (13). M cells in the terminal rectum of cattle have been demonstrated to express vimentin as the predominant intermediate filament protein (49), and the same staining was apparent in the cultured primary cells. A subset of vimentin-expressing cells was also able to take up *S.* Typhimurium (Fig. 5D) alone and *S.* Typhimurium and beads together (Fig. 5E). Therefore, the bovine rectal primary cultures contain a subset of cells that express vimentin and have characteristics of M cells. There was a significant role for *espF* in inhibiting bacterial uptake into cells, and translocation through these cells and the activity of the strains correlated with that of the *espF* alleles. An important result was that, in contrast to the previous experiments on mouse macrophages and the human-derived M-cell coculture system, EHEC O157 was the most effective strain at inhibiting uptake and translocation and this correlated with the relative activity of the *espF* alleles (Fig. 6). Taken together, these results indicate that EHEC O157 and the $espF_{O157}$ allele are more effective at inhibiting uptake into bovine M cells than the O26 and O127 strains and alleles, a reversal of the situation observed for the interactions with murine macrophages and the human coculture system.

There are multiple phenotypes associated with EspF in addition to inhibition of phagocytosis, including inhibition of water transport and disruption of tight junctions mitochondria and the nucleolus (17, 29, 58, 80). Uptake functions are likely to be related to EspF interactions with N-WASP and SNX9 (1). N-WASP stimulates actin filament assembly by direct activation of the Arp2/3 complex, and SNX9 is essential for clathrin-coated pits (CCPs) at the late stages of vesicle formation. SNX9 binds to β2 appendages of adaptor protein complex 2 (AP-2) and interacts with clathrin and dynamin-2, two other important molecules in the endocytic process (48, 77). SNX9 has two lipid interaction domains; a phospholipid-bind-

ing region termed the phox (PX) domain, followed by a putative Bin/amphiphysin/Rvs (BAR) lipid-binding domain. The BAR domain is a banana-shaped helical dimer that senses membrane curvature and can reconfigure lipid vesicles or sheets into membrane tubules (1). SNX9 also possesses an N-terminal Src homology-3 (SH3) protein interaction region that was recently shown to bind WASP (2) and to functionally activate dynamin at CCPs. Therefore, SNX9 is an important factor in remodeling the membrane and cytoskeletal during endocytosis (1, 77). The SH3 domain of SNX9 binds to the PPRs of EspF (1, 17). Despite both direct and indirect (via SNX9) activation of N-WASP, EspF is not considered to have a role in A/E lesion formation (54, 55). To determine whether the different EspF variants have different affinities for SNX9 and N-WASP, the interactions were assayed inside transfected HEK293 cells using a LUMIER assay (4; described in Materials and Methods). This in-cell assay confirmed that all three EspF variants bound to both N-WASP and SNX9, although $EspF_{O157}$ showed a lower interaction score with both SNX9 and N-WASP compared to the other two variants. Whether this is due to a reduced affinity of $EspF_{O157}$ for these two proteins remains to be determined. A specific region in the PRRs of EspF (shaded gray in Fig. 2) interacts directly with SNX9 through its SH3 domain-binding motif. There are only minor differences in this region between the serotypes examined here, and we cannot determine whether these or their presentation, due to sequence changes in flanking regions, account for the differences observed.

The published *Bos taurus* sequence for SNX9 (NCBI) contains a number of changes over the human variant used in the LUMIER assays; however, these differences are mainly present in the amino terminus of the predicted bovine SNX9 and lie outside the SH3 domain. There are also very few sequence differences between the predicted *Bos taurus* N-WASP protein sequence (NCBI) and the human variant. Taken together, our results indicate that there are likely to be other protein interactions involving EspF that could also contribute to the host specificity demonstrated here. The greatest region of diversity between the variants lies in the motifs preceding the second and third PRRs (amino acids 110 to 118 and amino acids 157 to 165 in Fig. 2), with no established function for these regions. Future work will seek to identify other interacting partners for EspF and address how important M-cell interactions are for colonization of cattle at the terminal rectum or whether other factors may explain the tropism of the EHEC O157:H7 for this gastrointestinal site.

ACKNOWLEDGMENTS

A.T. thanks the Egyptian government for Ph.D. research support. D.L.G. and A.M. acknowledge the core support of the BBSRC at the Roslin Institute. K.S. was funded by a research grant from the BBSRC (15/D19613).

REFERENCES

1. **Alto, N. M., et al.** 2007. The type III effector EspF coordinates membrane trafficking by the spatiotemporal activation of two eukaryotic signaling pathways. J. Cell Biol. **178:**1265–1278.
2. **Badour, K., et al.** 2004. Fyn and PTP-PEST-mediated regulation of Wiskott-Aldrich syndrome protein (WASp) tyrosine phosphorylation is required for coupling T cell antigen receptor engagement to WASp effector function and T cell activation. J. Exp. Med. **199:**99–112.
3. **Bai, Y., Y. Muragaki, K. Obata, K. Iwata, and A. Ooshima.** 1986. Immunological properties of monoclonal antibodies to human and rat prolyl 4-hydroxylase. J. Biochem. **99:**1563–1570.
4. **Barrios-Rodiles, M., et al.** 2005. High-throughput mapping of a dynamic signaling network in mammalian cells. Sci. STKE **307:**1621–1625.
5. **Bettelheim, K. A.** 2000. Role of non-O157 VTEC. Symp. Ser. Soc. Appl. Microbiol. **29:**38S–50S.
6. **Beutin, L.** 2006. Emerging enterohaemorrhagic *Escherichia coli*: causes and effects of the rise of a human pathogen. J. Vet. Med. Ser. B **53:**299–305.
7. **Booth, C., S. Patel, G. Bennion, and C. Potten.** 1995. The isolation and culture of adult mouse colonic epithelium. Epithelial Cell Biol. **4:**76–86.
8. **Boyce, T. G., D. L. Swerdlow, and P. M. Griffin.** 1995. *Escherichia coli* O157:H7 and the hemolytic-uremic syndrome. N. Engl. J. Med. **333:**364–368.
9. **Braun, P., et al.** 2008. An experimentally derived confidence score for binary protein-protein interactions. Nat. Methods **6:**91–97.
10. **Campellone, K. G., et al.** 2007. Increased adherence and actin pedestal formation by dam-deficient enterohaemorrhagic *Escherichia coli* O157:H7. Mol. Microbiol. **63:**1468–1481.
11. **Celli, J., M. Olivier, and B. B. Finlay.** 2001. Enteropathogenic *Escherichia coli* mediates antiphagocytosis through the inhibition of PI 3-kinase-dependent pathways. EMBO J. **20:**1245–1258.
12. **Choy, M., J. Walker-Smith, C. Williams, and T. MacDonald.** 1990. Differential expression of CD25 (interleukin-2 receptor) on lamina propria T cells and macrophages in the intestinal lesions in Crohn's disease and ulcerative colitis. Gut **31:**1365–1370.
13. **Clark, M., M. Jepson, N. Simmons, T. Booth, and B. Hirst.** 1993. Differential expression of lectin-binding sites defines mouse intestinal M cells. J. Histochem. Cytochem. **41:**1679–1687.
14. **Clark, M., M. Jepson, N. Simmons, and B. Hirst.** 1994. Preferential interaction of *Salmonella typhimurium* with mouse Peyer's patch M cells. Microbiol. Res. **145:**543–552.
15. **Crane, J. K., B. P. McNamara, and M. S. Donnenberg.** 2001. Role of EspF in host cell death induced by enteropathogenic *Escherichia coli*. Cell. Microbiol. **3:**197–211.
16. **Dean, P., M. Maresca, S. Schüller, A. D. Phillips, and B. Kenny.** 2006. Potent diarrheagenic mechanism mediated by the cooperative action of three enteropathogenic *Escherichia coli*-injected effector proteins. Proc. Natl. Acad. Sci. U. S. A. **103:**1876–1881.
17. **Dean, P., et al.** 2010. The enteropathogenic *E. coli* effector EspF targets and disrupts the nucleolus by a process regulated by mitochondrial dysfunction. PLoS Pathog. **6:**119–127.
18. **Dong, N., L. Liu, and F. Shao.** 2010. A bacterial effector targets host DH-PH domain RhoGEFs and antagonizes macrophage phagocytosis. EMBO J. **29:**1363–1376.
19. **Echtenkamp, F., et al.** 2008. Characterization of the NleF effector protein from attaching and effacing bacterial pathogens. FEMS Microbiol. Lett. **281:**98–107.
20. **Elliott, S. J., et al.** 2002. A gene from the locus of enterocyte effacement that is required for enteropathogenic *Escherichia coli* to increase tight-junction permeability encodes a chaperone for EspF. Infect. Immun. **70:**2271–2277.
21. **Ermak, T., H. Bhagat, and J. Pappo.** 1994. Lymphocyte compartments in antigen-sampling regions of rabbit mucosal lymphoid organs. Am. J. Trop. Med. Hyg. **50:**14–28.
22. **Farstad, I., T. Halstensen, O. Fausa, and P. Brandtzaeg.** 1994. Heterogeneity of M-cell-associated B and T cells in human Peyer's patches. Immunol. **83:**457–464.
23. **Frauli, M., and H. Ludwig.** 1987. Inhibition of fibroblast proliferation in a culture of human endometrial stromal cells using a medium containing D-valine. Arch. Gynecol. Obstet. **241:**87–96.
24. **Frey, A., et al.** 1996. Role of the glycocalyx in regulating access of microparticles to apical plasma membranes of intestinal epithelial cells: implications for microbial attachment and oral vaccine targeting. J. Exp. Med. **184:**1045–1059.
25. **Gebert, A., S. Fassbender, K. Werner, and A. Weissferdt.** 1999. The development of M cells in Peyer's patches is restricted to specialized dome-associated crypts. Am. J. Pathol. **154:**1573–1580.
26. **Giannasca, P., K. Giannasca, P. Falk, J. Gordon, and M. Neutra.** 1994. Regional differences in glycoconjugates of intestinal M cells in mice: potential targets for mucosal vaccines. Am. J. Physiol. Gastrointest. Liver Physiol. **267:**G1108–G1121.
27. **Giannasca, P., K. Giannasca, A. Leichtner, and M. Neutra.** 1999. Human intestinal M cells display the sialyl Lewis A antigen. Infect. Immun. **67:**946–953.
28. **Griffin, P. M., and R. V. Tauxe.** 1991. The epidemiology of infections caused by *Escherichia coli* O157:H7, other enterohemorrhagic *E. coli*, and the associated haemolytic-uraemic syndrome. Epidemiol. Rev. **13:**60–98.
29. **Guttman, J. A., and B. B. Finlay.** 2009. Tight junctions as targets of infectious agents. Biochim. Biophys. Acta **1788:**832–841.
30. **Hoey, D., et al.** 2003. Verotoxin 1 binding to intestinal crypt epithelial cells results in localization to lysosomes and abrogation of toxicity. Cell. Microbiol. **5:**85–97.
31. **Howard, C., P. Sopp, G. Bembridge, J. Young, and K. Parsons.** 1993. Com-

parison of CD1 monoclonal antibodies on bovine cells and tissues. Vet. Immunol. Immunopathology **39:**77–83.
32. **Howard, C., P. Sopp, K. Parsons, and J. Finch.** 1989. In vivo depletion of BoT4 (CD4) and of non-T4/T8 lymphocyte subsets in cattle with monoclonal antibodies. Eur. J. Immunol. **19:**757–764.
33. **Hueck, C. J.** 1998. Type III protein secretion systems in bacterial pathogens of animals and plants. Microbiol. Mol. Biol. Rev. **62:**379–433.
34. **Iizumi, Y., et al.** 2007. The enteropathogenic *Escherichia coli* effector EspB facilitates microvillus effacing and antiphagocytosis by inhibiting myosin function. Cell Host Microbe **2:**383–392.
35. **Iwasaki, A., and B. Kelsall.** 2000. Localization of distinct Peyer's patch dendritic cell subsets and their recruitment by chemokines macrophage inflammatory protein (MIP)-3, MIP-3, and secondary lymphoid organ chemokine. J. Exp. Med. **191:**1381–1394.
36. **Jarvis, K. G., et al.** 1995. Enteropathogenic *Escherichia coli* contains a putative type III secretion system necessary for the export of proteins involved in attaching and effacing lesion formation. Proc. Natl. Acad. Sci. U. S. A. **92:**7996–8000.
37. **Jensen, V. B., J. T. Harty, and B. D. Jones.** 1998. Interactions of the invasive pathogens *Salmonella typhimurium*, *Listeria monocytogenes*, and *Shigella flexneri* with M cells and murine Peyer's patches. Infect. Immun. **66:**3758–3766.
38. **Jepson, M. A., C. B. Collares-Buzato, M. A. Clark, B. H. Hirst, and N. L. Simmons.** 1995. Rapid disruption of epithelial barrier function by *Salmonella typhimurium* is associated with structural modification of intercellular junctions. Infect. Immun. **63:**356–359.
39. **Karch, H., P. I. Tarr, and M. Bielaszewska.** 2005. Enterohaemorrhagic *Escherichia coli* in human medicine. Int. J. Med. Microbiol. **295:**405–418.
40. **Karmali, M. A.** 2004. Infection by Shiga toxin-producing *Escherichia coli*. Mol. Biotechnol. **26:**117–122.
41. **Karmali, M. A.** 1989. Infection by verocytotoxin-producing *Escherichia coli*. Clin. Microbiol. Rev. **2:**15–38.
42. **Kenny, B., et al.** 1997. Enteropathogenic *E. coli* (EPEC) transfers its receptor for intimate adherence into mammalian cells. Cell **91:**511–520.
43. **Kenny, B., et al.** 2002. Co-ordinate regulation of distinct host cell signaling pathways by multifunctional enteropathogenic *Escherichia coli* effector molecules. Mol. Microbiol. **44:**1095–1107.
44. **Kerneis, S., A. Bogdanova, J. P. Kraehenbuhl, and E. Pringault.** 1997. Conversion by Peyer's patch lymphocytes of human enterocytes into M cells that transport bacteria. Science **277:**949–952.
45. **Kohbata, S., H. Yokoyama, and E. Yabuuchi.** 1986. Cytopathogenic effect of *Salmonella typhi* GIFU 10007 on M cells of murine ileal Peyer's patches in ligated ileal loops: an ultrastructural study. Microbiol. Immunol. **30:**1225–1237.
46. **Lazzaro, V., et al.** 1992. Inhibition of fibroblast proliferation in L-valine reduced selective media. Res. Com. Chem. Pathol. Pharmacol. **75:**39–48.
47. **Lo, D., et al.** 2004. Cell culture modeling of specialized tissue: identification of genes expressed specifically by follicle-associated epithelium of Peyer's patch by expression profiling of Caco-2/Raji cocultures. Int. Immunol. **16:**91–99.
48. **Lundmark, R., and S. R. Carlsson.** 2003. Sorting nexin 9 participates in clathrin-mediated endocytosis through interactions with the core components. J. Biol. Chem. **278:**46772–46781.
49. **Mahajan, A., et al.** 2005. Phenotypic and functional characterization of follicle-associated epithelium of rectal lymphoid tissue. Cell Tissue Res. **321:**365–374.
50. **Mairena, E. C., B. C. Neves, L. R. Trabulsi, and W. P. Elias.** 2004. Detection of LEE4 region-encoded genes from different enteropathogenic and enterohemorrhagic *Escherichia coli* serotypes. Curr. Microbiol. **48:**412–418.
51. **Marchès, O., et al.** 2006. EspF of enteropathogenic *Escherichia coli* binds sorting nexin 9. J. Bacteriol. **188:**3110–3115.
52. **Marchès, O., et al.** 2008. EspJ of enteropathogenic and enterohaemorrhagic *Escherichia coli* inhibits opsono-phagocytosis. Cellular Microbiol. **10:**1104–1115.
53. **Martinez-Argudo, I., C. Sands, and M. A. Jepson.** 2007. Translocation of enteropathogenic *Escherichia coli* across an in vitro M cell model is regulated by its type III secretion system. Cell. Microbiol. **9:**1538–1546.
54. **McNamara, B., et al.** 2001. Translocated EspF protein from enteropathogenic *Escherichia coli* disrupts host intestinal barrier function. J. Clin. Invest. **107:**621–629.
55. **McNamara, B. P., and M. S. Donnenberg.** 1998. A novel proline-rich protein, EspF, is secreted from enteropathogenic *Escherichia coli* via the type III export pathway. FEMS Microbiol. Lett. **166:**71–78.
56. **Moon, H., S. Whipp, R. Argenzio, M. Levine, and R. Giannella.** 1983. Attaching and effacing activities of rabbit and human enteropathogenic *Escherichia coli* in pig and rabbit intestines. Infect. Immun. **41:**1340–1351.
57. **Naessens, J., and C. Howard.** 1991. Monoclonal antibodies reacting with bovine B cells (BoWC3, BoWC4, and BoWC5). Vet. Immunol. Immunopathol. **27:**77–85.
58. **Nagai, T., A. Abe, and C. Sasakawa.** 2005. Targeting of enteropathogenic *Escherichia coli* EspF to host mitochondria is essential for bacterial pathogenesis. J. Biol. Chem. **280:**2998–3011.
59. **Naylor, S. W., D. L. Gally, and J. Christopher Low.** 2005. Enterohemorrhagic *Escherichia coli* in veterinary medicine. Int. J. Med. Microbiol. **295:**419–441.
60. **Naylor, S. W., et al.** 2003. Lymphoid follicle-dense mucosa at the terminal rectum is the principal site of colonization of enterohemorrhagic *Escherichia coli* O157: H7 in the bovine host. Infect. Immun. **71:**1505–1512.
61. **Naylor, S. W., A. J. Roe, P. Nart, K. Spears, and D. Smith.** 2005. *Escherichia coli* O157:H7 forms attaching and effacing lesions at the terminal rectum of cattle and colonization requires the LEE4 operon. Microbiology **151:**2773–2781.
62. **Neutra, M., E. Pringault, and J. Kraehenbuhl.** 1996. Antigen sampling across epithelial barriers and induction of mucosal immune responses. Annu. Rev. Immunol. **14:**275–300.
63. **Norimatsu, M., et al.** 2003. Differential response of bovine monocyte derived macrophages and dendritic cells to infection with *Salmonella typhimurium* in a low dose model *in vitro*. Immunology **108:**55–61.
64. **Nougayrede, J., et al.** 2001. Type III secretion-dependent cell cycle block caused in HeLa cells by enteropathogenic *Escherichia coli* O103. Infect. Immun. **69:**6785–6795.
65. **Nougayrède, J. P., and M. S. Donnenberg.** 2004. Enteropathogenic *Escherichia coli* EspF is targeted to mitochondria and is required to initiate the mitochondrial death pathway. Cell. Microbiol. **6:**1097–1111.
66. **Nougayrède, J. P., G. H. Foster, and M. S. Donnenberg.** 2007. Enteropathogenic *Escherichia coli* effector EspF interacts with host protein Abcf2. Cell. Microbiol. **9:**680–693.
67. **Owen, R.** 1999. Uptake and transport of intestinal macromolecules and microorganisms by M cells and Peyer's patches: a historical and personal perspective. Semin. Immunol. **11:**157–163.
68. **Owen, R., and D. Bhalla.** 1983. Cytochemical analysis of alkaline phosphatase and esterase activities and of lectin-binding and anionic sites in rat and mouse Peyer's patch M cells. Am. J. Anat. **168:**199–212.
69. **Pomposiello, P., M. Bennik, and B. Demple.** 2001. Genome-wide transcriptional profiling of the *Escherichia coli* responses to superoxide stress and sodium salicylate. J. Bacteriol. **183:**3890–3920.
70. **Quitard, S., P. Dean, M. Maresca, and B. Kenny.** 2006. The enteropathogenic *Escherichia coli* EspF effector molecule inhibits PI-3 kinase-mediated uptake independently of mitochondrial targeting. Cell. Microbiol. **8:**972–981.
71. **Roe, A., et al.** 2007. Analysis of the expression, regulation and export of NleA-E in *Escherichia coli* O157:H7. Microbiol. **153:**1350–1360.
72. **Savidge, T.** 1996. The life and times of an intestinal M cell. Trends Microbiol. **4:**301–306.
73. **Savidge, T., and M. Smith.** 1995. Evidence that membranous (M) cell genesis is immuno-regulated. Adv. Exp. Med. Biol. **371:**239–241.
74. **Shaw, R. K., J. Cleary, M. S. Murphy, G. Frankel, and S. Knutton.** 2005. Interaction of enteropathogenic *Escherichia coli* with human intestinal mucosa: role of effector proteins in brush border remodeling and formation of attaching and effacing lesions. Infect. Immun. **73:**1243–1251.
75. **Smith, M., and M. Peacock.** 1980. "M" cell distribution in follicle-associated epithelium of mouse Peyer's patch. Am. J. Anat. **159:**167–175.
76. **Sörensen, M., et al.** 2003. Rapidly maturing red fluorescent protein variants with strongly enhanced brightness in bacteria. FEBS Lett. **552:**110–114.
77. **Soulet, F., D. Yarar, M. Leonard, and S. L. Schmid.** 2005. SNX9 regulates dynamin assembly and is required for efficient clathrin-mediated endocytosis. Mol. Biol. Cell **16:**2058–2067.
78. **Teale, A., C. Baldwin, W. Morrison, J. Ellis, and N. MacHugh.** 1987. Phenotypic and functional characteristics of bovine T lymphocytes. Vet. Immunol. Immunopathol. **17:**113–123.
79. **Tobe, T., et al.** 2006. An extensive repertoire of type III secretion effectors in *Escherichia coli* O157 and the role of lambdoid phages in their dissemination. Proc. Natl. Acad. Sci. U. S. A. **103:**14941–14946.
80. **Viswanathan, V., et al.** 2004. Comparative analysis of EspF from enteropathogenic and enterohemorrhagic *Escherichia coli* in alteration of epithelial barrier function. Infect. Immun. **72:**3218–3227.

Editor: B. A. McCormick